Article

Response of Triticum Vulgare Growth and Nitrogen Allocation to Irrigation Methods and Regimes under Subsoiling Tillage

Chao Huang [1,2,3,4,†], Xuchen Liu [1,2,3,4,†], Yang Gao [1,2], Haiqing Chen [1,2,3], Shoutian Ma [1,2,3], Anzhen Qin [1,2,3], Yingying Zhang [1,3], Zile Gao [5], Yan Song [5], Jinkai Sun [5] and Zhandong Liu [1,2,3,*]

1   Institute of Farmland Irrigation, Chinese Academy of Agriculture Sciences, Xinxiang 453003, China; huangchao_124@126.com (C.H.); finaloo@163.com (X.L.); gaoyang@caas.cn (Y.G.); chqboss@163.com (H.C.); mashoutian@caas.cn (S.M.); qinanzhen@caas.cn (A.Q.); hdzyy155@163.com (Y.Z.)
2   Western Agricultural Research Center, Chinese Academy of Agricultural Sciences, Changji 831100, China
3   Henan Agricultural Efficient Water Field Scientific Observation and Research Station, Xinxiang 453003, China
4   Graduate School of Chinese Academy of Agricultural Sciences, Beijing 100081, China
5   Henan Yudong Water Conservancy Security Center, Kaifeng 475000, China; gaozile99111@163.com (Z.G.); syzsy1984@163.com (Y.S.); sunjinkai1987@sohu.com (J.S.)
*   Correspondence: liuzhandong@caas.cn
†   These authors contributed equally to this work.

Abstract: Subsoiling tillage breaks up the shallow plow layer and thickened plow pan resulting from prolonged crop rotation, thus enhancing the soil tillage layer environment and fostering crop growth. However, these changes in tillage practices are not accompanied by corresponding advancements in irrigation technology. Therefore, this study compared drip irrigation (DI) and micro-sprinkler irrigation (MS) with three watering levels (H, M, L) based on soil water content (70%, 60%, 50% of field capacity) against traditional surface irrigation (CK, 70%FC) to find the most suitable irrigation approach for subsoiling wheat fields. This study found that adjusting irrigation methods and regimes significantly impacted wheat growth and yield. Drip irrigation boosts winter wheat grain yield, harvest index, biomass transfer amount, biomass transfer rate, nitrogen accumulation, nitrogen use efficiency, and nitrogen harvest index significantly compared to surface and micro-sprinkler methods. Drip irrigation, notably the DI-M treatment, significantly enhances winter wheat grain yield by 28.7% compared to CK. Drip irrigation produced optimal results when soil water levels decreased to 60% of the field capacity. This suggests adopting a combination of DI, with irrigation initiated at 60% of field capacity, for enhanced wheat production and resource efficiency.

Keywords: winter wheat; drip/micro-sprinkler irrigation; irrigation regime; biomass transfer amount; nitrogen accumulation

1. Introduction

The Huang–Huai–Hai Plain plays a crucial role in China's grain production as the nation's primary winter wheat-producing region. However, with the development of the agricultural economy, agricultural mechanization has been widely adopted, and the weight of agricultural machinery continues to increase, leading to soil compaction in crops [1]. Additionally, frequent continuous tillage practices in most parts of the Huaihe–Huai Plain have resulted in deep soil compaction, thickening of the plow pan layer, and shallower plow layer formation. In the Huang–Huai–Hai Plain's northern region, the plow layer soil averages only 14.7 cm thick. The 15–35 cm layer is predominantly the plow pan layer, with a bulk density of 1.6 g·cm^{-3}, notably exceeding the optimal range for crop growth (1.1–1.3 g·cm^{-3}) [2,3]. Additionally, the poor plow layer structure weakens the functions of coordinating soil water, fertilizer, air, and heat, resulting in a shallow distribution of crop roots and significant limitations on water and nutrient absorption [4]. Constructing a reasonable plow layer structure through appropriate tillage practices is an important

approach to improving crop water and nutrient utilization efficiency and enhancing soil productivity [5].

Studies suggest that subsoiling effectively disrupts the plow pan layer, leading to improved soil permeability, increased water retention capacity, and enhanced resilience to adverse conditions. These benefits create a conducive soil plow layer environment for crop growth, fostering crop development and ultimately increasing yield [6]. Subsoiling accomplishes this by decreasing soil bulk density, enhancing soil porosity, and promoting the infiltration of irrigation and rainfall, thereby reducing surface runoff and minimizing inefficient evaporation. Consequently, it enhances soil water and rainfall storage and fortifies soil buffering capacity against drought, with more pronounced effects observed during drier periods [7]. However, it is noteworthy that some studies have found that subsoiling, by disrupting the plow pan layer, may increase leaching, thereby potentially reducing soil water storage capacity and the availability of soil nutrients [8]. This phenomenon could be attributed to the plow pan layer's role in minimizing water percolation loss and nutrient leaching loss, thereby providing a certain level of water and nutrient retention effect.

Irrigation stands as a pivotal agronomic management practice crucial for ensuring high and consistent yields of winter wheat, directly influencing soil structure and the dynamics of water and nutrient movement, thereby impacting aboveground plant growth [9]. Traditional surface irrigation methods often contribute to detrimental effects on soil aggregates, resulting in surface sealing. Conversely, micro-irrigation, particularly drip irrigation, demonstrates the capacity to improve the stability of soil micro-aggregates and preserve soil structure [10]. Drip irrigation, being a prominent water-saving irrigation technology, offers the advantage of conserving water and fertilizer resources [11]. Drip irrigation enhances water use efficiency and changes the distribution of water, nutrients, and roots in the soil by delivering precise amounts of nutrients and water directly to the crop root zone [11–13]. Research indicates that drip irrigation leads to increased root density in wheat plants, facilitating enhanced root water and nutrient absorption, and consequently improving crop productivity [12,13]. Moreover, drip irrigation contributes to bolstering crop photosynthesis, promoting dry matter accumulation, and ultimately boosting crop productivity [14–16]. Micro-sprinkler irrigation, another water-saving micro-irrigation method, has been shown to elevate the chlorophyll content of winter wheat, retard leaf aging, enhance net photosynthetic rate and electron transfer in photosynthesis, and diminish intercellular CO_2 concentration, transpiration rate, and leaf stomatal conductance, thereby furnishing ample dry matter for grain formation [17]. Comparative analyses indicate that micro-sprinkler irrigation, in contrast to surface irrigation, conserves water by 9–11%, augments yield by 6–11%, and enhances crop water productivity [18,19]. Furthermore, irrigation methods can be integrated with fertilization, yielding benefits such as increased wheat yield, enhanced fertilizer utilization, augmented soil carbon storage, and reduced greenhouse gas emissions from farmland [20,21]. Fertilization in conjunction with drip irrigation has been found to enhance water and nutrient absorption, elevate nitrogen fertilizer utilization efficiency, and effectively curtail nitrogen leaching losses, reducing deep leaching losses of nitrate nitrogen by 90% [20,22–24].

In the Huang–Huai–Hai region, while surface irrigation remains prevalent, water-saving irrigation technologies, like drip irrigation and micro-sprinklers, are swiftly gaining traction, gradually supplanting traditional flood irrigation methods. Given the evolving farming practices, traditional irrigation approaches no longer align with subsoiling tillage techniques. Will water-saving irrigation methods improve the accumulation of dry matter and post-flowering dry matter transfer in winter wheat? Can they enhance winter wheat's nitrogen utilization efficiency? These questions deserve widespread attention. This study aims to explore the effects of various irrigation methods and regimes on the post-anthesis biomass accumulation and transfer processes of winter wheat under subsoiling tillage conditions. Its primary aims encompass elucidating the nitrogen utilization efficiency of winter wheat and identifying the optimal irrigation method and regime for its cultivation under subsoiling tillage. The insights gleaned from this study are poised to furnish a crucial

theoretical foundation and empirical evidence for devising appropriate irrigation and fertilization management systems tailored to winter wheat cultivation under subsoiling tillage. Such advancements hold significant theoretical and practical implications in facilitating the attainment of environmentally sustainable and efficiently augmented winter wheat yields under subsoiling tillage practices.

2. Materials and Methods

2.1. Experimental Site

The experiment took place at the Xinxiang Comprehensive Experimental Base of the Chinese Academy of Agricultural Sciences, situated in Qiliying, Xinxiang, Henan Province. This study spanned from October 2020 to June 2022 (35.15° N, 113.80° E, altitude 81 m). The area falls within a temperate semi-humid climate zone, is prone to drought, and serves as a significant production hub for winter wheat within the Huang–Huai–Hai Plain. The cropping system is primarily based on a rotation of winter wheat and summer maize. The region receives an average annual precipitation of 582 mm and experiences an average annual temperature of 14 °C. The groundwater depth is greater than 5 m, with a frost-free period of 210 days. The soil at the experimental site originates from the alluvial sediments of the Yellow River and is categorized as Aquic Ustochrept, a type of paddy soil, under the USDA soil taxonomy [25]. It exhibits a sandy loam texture, comprising 57.3% sand, 4.05% clay, and 38.6% silt. Soil physicochemical properties of the 0–40 cm soil layer are shown in Table 1.

Table 1. The fundamental soil parameters within the 0–40 cm soil layer of the experimental field for winter wheat.

Location	Soil Texture	Soil Dry Bulk Density	Soil Field Capacity	Organic Matter	Total Nitrogen	Available Phosphorus	Available Potassium
		/g·cm^{-3}	/cm^3·cm^{-3}	/g·kg^{-1}	/g·kg^{-1}	/mg·kg^{-1}	/mg·kg^{-1}
Xinxiang	Silt loam soil	1.51	0.31	16.1	1.05	23.4	229.5

Near the experimental site, a weather station (YM-HJ03, Handan Chuangmeng Electronic Technology Company Limited, Handan, China) was installed. It recorded cumulative rainfall of 172 mm and 60 mm during the winter wheat growing seasons, respectively. Daily average temperatures and daily precipitation are shown in Table 2.

Table 2. Meteorological parameters for each month of two winter wheat growing seasons.

Year	Month	Air Humidity	Total Radiation	Precipitation	T$_{max}$	T$_{min}$
		/%	/W·m^{-2}	/mm	/°C	/°C
2020–2021	October	76.44	1914.19	20.70	20.32	9.33
	November	79.16	2389.85	70.50	14.36	6.03
	December	22.90	2439.16	4.00	2.60	0.00
	January	55.74	2999.73	0.00	7.88	−2.90
	February	68.44	3398.56	54.10	13.69	1.87
	March	80.24	4014.15	14.40	15.45	7.22
	April	74.35	5542.67	29.60	20.27	10.11
	May	66.12	7463.01	12.10	28.09	15.44
	June	66.66	591.73	0.00	31.68	20.35
2021–2022	October	78.49	220.55	0.00	22.90	10.40
	November	66.70	3700.98	18.90	16.00	5.02
	December	42.51	3486.86	3.70	2.49	0.00
	January	88.30	1894.89	12.60	4.81	−1.51
	February	69.81	3353.59	0.00	8.25	−1.71
	March	75.55	4124.46	10.80	15.94	6.25
	April	71.40	5677.78	9.10	23.04	10.91
	May	64.59	7508.74	35.40	27.31	14.85
	June	29.41	290.61	0.00	0.07	34.68

Note: T$_{max}$ represents the average monthly maximum temperature, while T$_{min}$ represents the average monthly minimum temperature.

2.2. Experimental Design

This study uses Zhoumai 22 as the experimental variety, with a seeding rate of 210 kg·ha^{-1} and a row spacing of 20 cm for winter wheat, and the previous crop of wheat is summer maize. Planting was conducted on 13 October 2020 and 30 October 2021, with harvests on 4 June 2021 and 6 June 2022. The parameters of the wheat seeder and harvester are shown in Tables S1 and S2. The experimental design involved two factors: irrigation method and irrigation regime. The experimental setup included two variables: irrigation method (drip irrigation—DI, micro-sprinkler irrigation—MS) and irrigation regimen (well watered—H, mild water deficit—M, and moderate water deficit—L), with irrigation thresholds set at 70%, 60%, and 50% of field capacity, respectively. Border irrigation at 70% of field capacity, representing the local conventional irrigation regime, serves as the control (CK). In total, there are 7 treatments, with each treatment plot measuring 50 × 13 m^2, subdivided into 3 subplots of 50 × 4.3 m^2 each, and these serve as 3 replicates. The specific experimental design is detailed in Table 3. The irrigation quotas for border irrigation, micro-sprinkler irrigation, and drip irrigation are 90 mm, 45 mm, and 30 mm, respectively.

Table 3. Irrigation experiment design of winter wheat.

Irrigation Method	Treatment	Lower Limit of Soil Moisture Control	Irrigating Quota
		/%FC	/mm
Border irrigation	CK	70	90
Drip irrigation	DI-H	70	30
	DI-M	60	30
	DI-L	50	30
Micro-sprinkler irrigation	MS-H	70	45
	MS-M	60	45
	MS-L	50	45

Note: The values in the table are the lower limit index of soil moisture control, which is the percentage of soil water in field capacity.

Tillage involved deep plowing to a depth of 35 cm once every two years on the day of winter wheat sowing. The parameters of the soil deep loosening machine are shown in Table S3. Subsoiling was conducted before sowing in 2020 and 2022. The spacing between drip irrigation emitters was 0.6 m, while the spacing between micro-sprinkler tape and between micro-sprinkler heads was 2 m. Each furrow plot measured 50 m in length and 3.4 m in width. Irrigation amounts were 30 mm for drip irrigation, 45 mm for micro-sprinkler irrigation, and 90 mm for surface irrigation when the lower limits were reached. The irrigation amount of each treatment during the whole growth period is shown in Table 4. Basic fertilization is carried out using urea (46.7% N), calcium superphosphate (16% P_2O_5), and potassium sulfate (50% K_2O) for nitrogen, phosphorus, and potassium, respectively. Prior to sowing, the fertilizers are spread on the surface and incorporated into the soil using a rotary tillage machine. A standard fertilization rate of 120 kg·ha^{-1} was utilized for phosphorus and potassium application. Nitrogen fertilizer was applied at a rate of 240 kg·ha^{-1}, with 40% applied as basic fertilizer and 60% as topdressing using fertigation during the regreening stage of wheat. Other field management measures are consistent with local agricultural practices.

Table 4. Irrigation amounts for two growing seasons of winter wheat under various irrigation methods and regimes.

Year	Irrigation Date	Irrigation Amount/mm						
		CK	DI-H	DI-M	DI-L	MS-H	MS-M	MS-L
2020–2021	November	0	30	30	30	45	45	45
	December	90	0	0	0	0	0	0
	March	90	60	30	30	90	45	45
	April	0	30	30	0	45	45	0
	May	90	30	30	0	45	45	0
	Total	270	150	120	60	225	180	90
2021–2022	December	90	30	30	30	45	45	45
	February	90	30	30	30	0	0	0
	March	90	30	0	0	90	45	45
	April	0	60	30	30	45	45	45
	May	90	30	30	0	45	45	0
	Total	360	180	120	90	225	180	135

2.3. Data Collection

2.3.1. Leaf Area Index and SPAD Value

During the winter wheat's jointing, flowering, and filling stages, the SPAD value of wheat flag leaves was measured using a portable SPAD-502 chlorophyll meter (Konica Minolta Holdings, Inc., Tokyo, Japan), with 7 plants measured per subplot. The leaf area index (*LAI*) was determined using the Sunscan Canopy Analysis System (Delta T Devices Ltd., Cambridge, UK).

2.3.2. Measurements of Gas Exchange

After the flowering stage, gas exchange parameters of winter wheat leaves were measured approximately every 7 days. Measurements were conducted using an Li-6400 portable photosynthesis system (LI-COR, Lincoln, NE, USA) between 9:00 and 11:00 a.m. on sunny days. Gas exchange parameters assessed included net photosynthetic rate (P_n), stomatal conductance (G_s), transpiration rate (T_r), and intercellular CO_2 concentration (C_i) of the flag leaves of winter wheat. Three plants were measured for each treatment.

2.3.3. Shoot Biomass and Its Distribution

During the flowering and maturity stages of winter wheat, aboveground biomass was measured for each treatment. Three replicates were taken for each treatment, with each replicate consisting of thirty plants. Additionally, the spike density per unit area was recorded. The biomass was determined by dividing the aboveground plant parts into leaves, stems, glumes, and grains. Subsequently, all samples were dried in an oven at 105 °C for 30 min, followed by drying at 75 °C until a constant weight was achieved. The aboveground biomass was then weighed to determine the distribution percentages of leaves, stems, glumes, and grains relative to the entire aboveground biomass. Referring to the study by Fan et al. [26], we calculated the biomass accumulation after flowering (BAF, kg·ha^{-1}), biomass transfer amount (BTA, kg·ha^{-1}) and its transfer rate (BTR, %), and the contribution rate of BTA from vegetative organs to grain (GCR, %) using Equations (1)–(4) as follows:

$$BAF = \text{Biomass at the maturity stage} - \text{Biomass at the flowering stage} \tag{1}$$

$$BTA = \text{Biomass at the flowering stage} - (\text{Biomass at the maturity stage} - \text{grain yield}) \tag{2}$$

$$BTR = \frac{BTA}{\text{Biomass at the flowering stage}} \times 100\% \tag{3}$$

$$\text{GCR} = \frac{\text{BTA}}{\text{Grain yield}} \times 100\% \tag{4}$$

2.3.4. Nitrogen Uptake and Its Utilization and Grain Yield

Nitrogen content in the leaves, stems, glumes, and grains of mature winter wheat was determined using the Kjeldahl method [27]. Referring to Qi et al. [28], nitrogen accumulation (NA, kg·ha^{-1}) in the aboveground parts was calculated using the biomass of each organ (Equation (5)), and nitrogen use efficiency (NUE, %; Equation (6)) and nitrogen harvest index (NHI, %; Equation (7)) were calculated using grain yield.

$$\text{NA} = W_{\text{leaf}} \times N_{\text{leaf}} + W_{\text{stem}} \times N_{\text{stem}} + W_{\text{glume}} \times N_{\text{glume}} + \text{GY} \times N_{\text{grain}} \tag{5}$$

$$\text{NUE} = \frac{\text{GY}}{\text{NA}} \tag{6}$$

$$\text{NHI} = \frac{\text{GY} \times N_{\text{grain}}}{\text{NA}} \tag{7}$$

where W_{leaf} is the leaf biomass (kg·ha^{-1}), N_{leaf} is the leaf nitrogen content (%), W_{stem} is the stem biomass (kg·ha^{-1}), N_{stem} is the stem nitrogen content (%), W_{glume} is the glume biomass (kg·ha^{-1}), N_{glume} is the glume nitrogen content (%), GY is the grain yield (kg·ha^{-1}), and N_{grain} is the grain nitrogen content (%).

2.3.5. Root Sampling

In the 2021–2022 growing seasons, at the maturity stage of winter wheat, root samples were collected across various soil depths (0–10 cm to 70–100 cm) using a root auger. Then, the root samples underwent scanning with an Epson V850 Pro root scanner (Epson, Nagano, Japan), followed by an analysis of the scanned images using WinRHIZO 2007 software (Regent Instruments, Québec City, QC, Canada). The analyzed root parameters included root length (cm), average diameter (mm), and volume (mm^3). Place the wheat roots in an oven at 105 °C to halt growth and dry them at 75 °C until a constant weight is achieved, and then measure the root dry weight (mg). Calculate the root length density, root volume density, and root dry weight density per cubic centimeter of depth unit.

2.3.6. TOPSIS Comprehensive Evaluation

The TOPSIS method was used to comprehensively evaluate the leaf area index (*LAI*), SPAD value, total biomass, harvest index (HI, %), grain yield (GY, kg·ha^{-1}), biomass accumulation after flowering, biomass transfer amount (BTA, kg·ha^{-1}), biomass transfer rate (BTR), contribution rate of transferred biomass to grain yield (GCR, %), nitrogen accumulation (NA, kg·ha^{-1}), nitrogen harvest index (NHI), and nitrogen use efficiency (NUE) of winter wheat at the maturity stage across seven treatments in two growing seasons [29].

2.4. Statistical Analysis

Excel 2019 (Microsoft Corporation, Redmond, WA, USA) was used to record data. Data were analyzed using one-way analysis of variance (ANOVA) in SPSS 19.0 (IBM Inc., Chicago, IL, USA), and the least significant difference (LSD) test was conducted to compare the means of different treatments at a 0.05 significance level. The TOPSIS method was used to comprehensively evaluate the experimental treatment. Origin 2016 (OriginLab Corporation, Northampton, MA, USA) was used to create the figures.

3. Results

3.1. The Response of Plant Growth of Winter Wheat Leaves to Irrigation Methods and Regimes

3.1.1. *LAI* and SPAD Value

The change patterns of the leaf area index (*LAI*) and *SPAD* value of winter wheat remain consistent over two growing seasons (Figure 1), both peaking during the flowering

stage. Under the same irrigation regime, winter wheat *LAI* under well-watered (H) and mild water deficit (M) treatments at the jointing stage, flowering stage, and maturity stage were significantly higher than those under moderate water deficit (L) treatment, demonstrating a trend of H ≥ M > L. Within the same irrigation method, during the flowering and maturity stages, the *LAI* and *SPAD* values of winter wheat followed the order of DI > MS > CK. Specifically, during the flowering stage, the *LAI* and *SPAD* values of the DI-H treatment increased by 11.2% and 7.7%, respectively, compared to the CK ($p < 0.05$), while during the maturity stage, the *LAI* and *SPAD* values of the DI-H treatment increased by 13.0% and 7.4%, respectively, compared to the CK ($p < 0.05$).
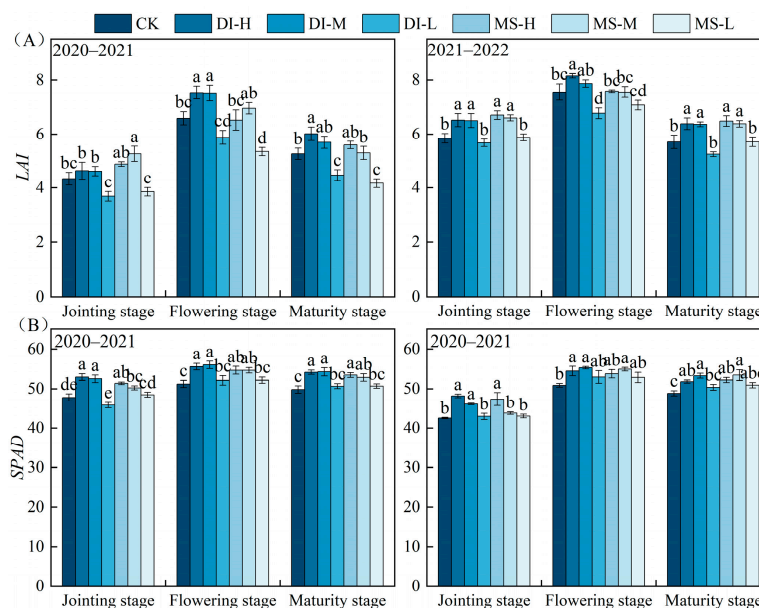
Figure 1. *LAI* (**A**) and *SPAD* (**B**) value of winter wheat during 2020–2022. (Note: different letters represent significant differences at the 0.05 level within the same growth stage. Error bars based on standard error (SE) were added to the data. Each data point was extended vertically by one standard error above and below the mean value).

3.1.2. Root Growth and Density

Under different irrigation methods and irrigation regimes, the root of winter wheat primarily concentrates in the 0–10 cm soil layer (Figure 2). Within the same irrigation method, drip irrigation (DI) shows an increase in root length density in the 0–10 cm soil layer with decreasing irrigation volume (Figure 2A), while the root length density in the 0–10 cm soil layer for micro-sprinkler irrigation (MS) is ranked as H > L > M. Under the same irrigation regime, the root length density in the 0–10 cm soil layer for the well-watered (H) treatment is ranked as MS-H > DI-H > CK. The root diameter of winter wheat did not exhibit significant differences across various soil layers under different irrigation methods and regimes (Figure 2B). However, the root volume density in the 0–10 cm soil layer for both DI and MS under different irrigation regimes showed no difference and was lower than the CK ($p < 0.05$; Figure 2C). Within the same irrigation method, the maximum root dry weight in the 0–10 cm soil layer was observed in the well-watered (H) treatment for DI (Figure 2D), while for MS, the moderate water deficit (L) treatment showed the maximum root dry weight. Under the same irrigation regime, the ranking of root dry weight in the 0–10 cm soil layer is CK > MS > DI. In conclusion, both root growth and dry matter accumulation under DI were slightly weaker compared to the CK and MS.
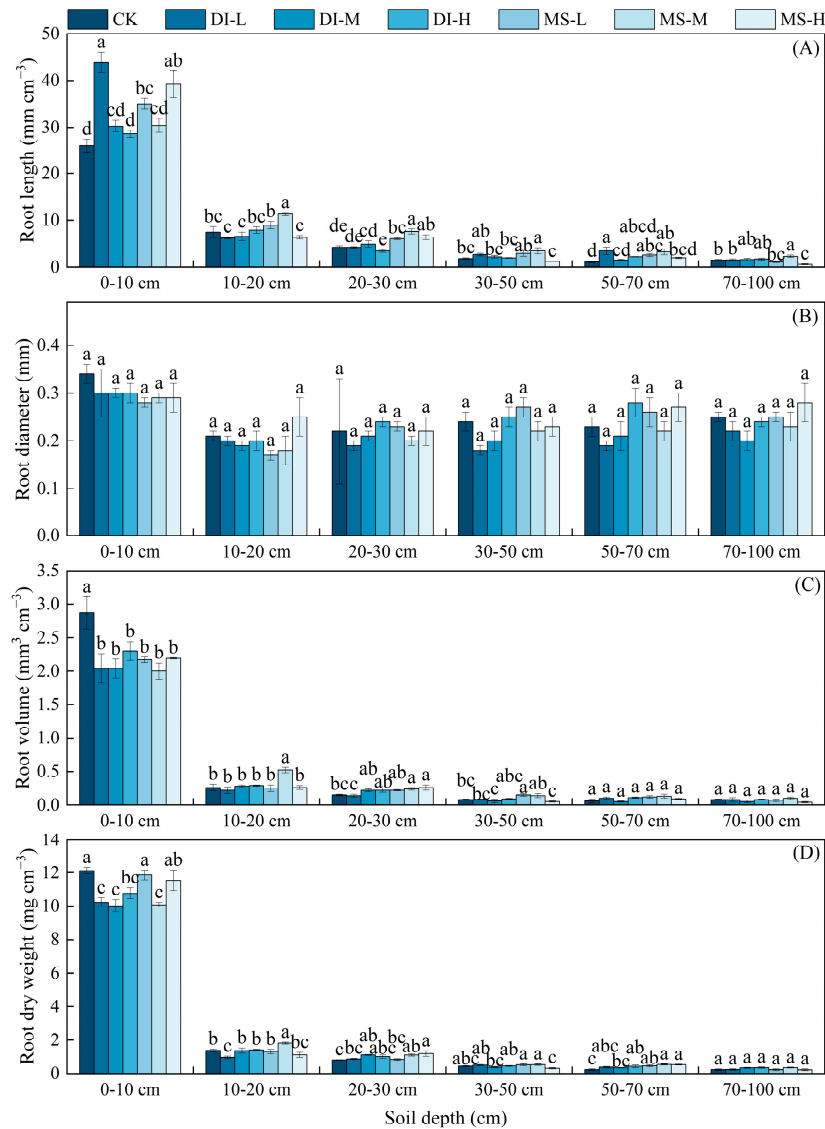
Figure 2. Root length density (**A**), root diameter (**B**), root volume density (**C**), and root dry weight density (**D**) of winter wheat during the 2021–2022 seasons. (Note: different letters indicate significant differences at the 0.05 level between different treatments at the same soil depth. Error bars based on standard error (SE) were added to the data. Each data point was extended vertically by one standard error above and below the mean value).

3.2. The Response of Photosynthetic Characteristics of Winter Wheat Leaves to Irrigation Methods and Regimes

The variation trends of stomatal conductance (G_s), intercellular CO_2 concentration (C_i), net photosynthetic rate (P_n), and stomatal conductance (T_r) in the leaves of winter wheat were generally consistent between the two growing seasons (Figure 3). Differences in stomatal conductance (G_s) among winter wheat leaves began to emerge after flowering under various irrigation methods and regimes. Within the same irrigation method, G_s decreased as water deficit intensity increased, with a 59.5% reduction in G_s for the DI-L treatment compared to the CK in late May ($p < 0.05$). Meanwhile, within the same irrigation regime, G_s during the mid-grain filling stage (mid-May) followed the pattern DI > MS ≥ CK (Figure 3A).
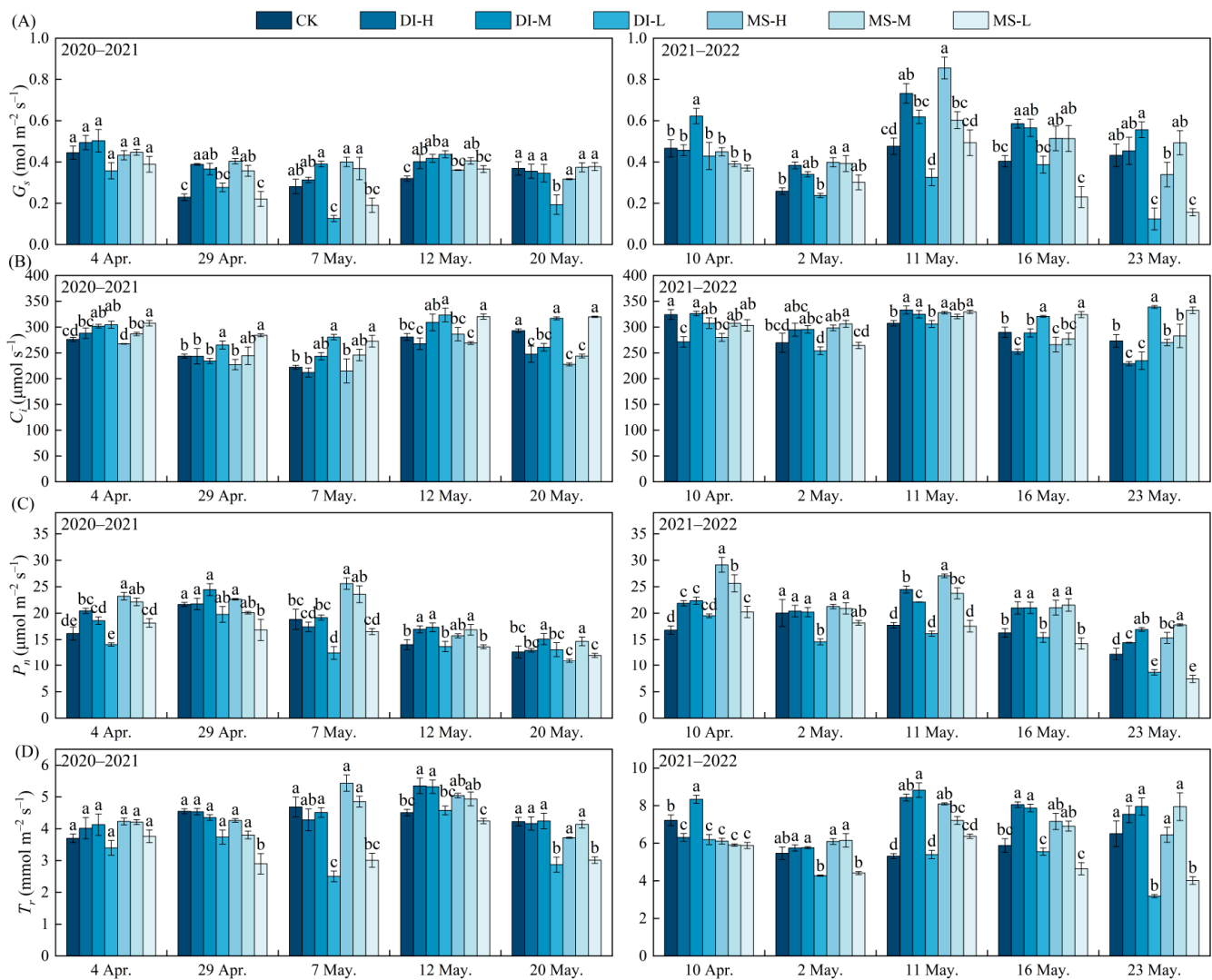
Figure 3. Stomatal conductance (G_s, mol·m^{-2}·s^{-1}) (**A**), intercellular CO_2 concentration (C_i, µmol·s^{-1}) (**B**), net photosynthetic rate (P_n, µmol·m^{-2}·s^{-1}) (**C**), and transpiration rate (T_r, mmol·m^{-2}·s^{-1}) (**D**) of winter wheat during the 2020–2022 seasons. (Note: when different letters appear alongside data points on the same date, it signifies notable variances at the 0.05 significance level. Error bars based on standard error (SE) were added to the data. Each data point was extended vertically by one standard error above and below the mean value).

Similarly, leaf intercellular CO_2 concentration (C_i) exhibited an increasing trend with water deficit intensity, while the photosynthetic rate (P_n) showed a decreasing trend (Figure 3B,C). In late May, the DI-M treatment showed the most significant reduction in C_i compared to the CK (decreased by 12.5%, $p < 0.05$), with the largest increase in P_n (increased by 28.7%, $p < 0.05$). Notably, C_i showed differences during the late grain filling stage (mid to late May) under the same irrigation regime, with the pattern CK > MS > DI, while P_n exhibited the pattern DI ≥ MS > CK. Moreover, the transpiration rate (T_r) of winter wheat leaves changed consistently with G_s. Under the same irrigation method, T_r decreased with increasing water deficit intensity after flowering, with reductions of 41.6% and 33.5% for the DI-L and MS-L treatments, respectively, compared to the CK in late May ($p < 0.05$). However, under the same irrigation regime, there was no difference in Tr between drip irrigation and micro-sprinkler irrigation, but both were significantly higher than conventional surface irrigation (Figure 3D). In summary, water deficit restricted the stomatal opening of winter wheat leaves during the grain filling stage, consequently

reducing the leaf photosynthetic rate. Notably, both DI and MS demonstrated superior photosynthetic characteristics compared to conventional surface irrigation.

3.3. The Response of Shoot Biomass of Winter Wheat to Irrigation Methods and Regimes

Consistency in the trends of the stem, leaf, glume, grain, and total biomass during the flowering and maturity stages of winter wheat was observed across both the 2020–2021 and 2021–2022 growing seasons (Table 5). Regardless of the irrigation method, the biomass of each organ and the total biomass of winter wheat decreased as water deficit intensity increased. However, during the flowering stage under the same irrigation regimen, the micro-sprinkler irrigation treatment displayed higher biomass in each organ compared to drip irrigation and the control (CK), resulting in an 11.4% increase in total biomass for the MS-H treatment compared to the CK ($p < 0.05$). In contrast, during the maturity stage, both drip irrigation and micro-sprinkler irrigation treatments exhibited higher grain yield and total biomass compared to CK. Grain yield increased by 27.0% and 15.8% for DI-H and MS-H treatments, respectively, compared to the CK ($p < 0.05$), while total biomass increased by 12.7% and 12.6% for DI-H and MS-H treatments, respectively ($p < 0.05$). Additionally, drip irrigation treatments demonstrated higher grain yield compared to micro-sprinkler irrigation treatments, indicating that drip irrigation facilitated the transfer of dry matter to grains.

Table 5. Stem biomass (kg·ha^{-1}), leaf biomass (kg·ha^{-1}), glume biomass (kg·ha^{-1}), grain yield (kg·ha^{-1}), and total biomass (kg·ha^{-1}) of winter wheat during the 2020–2022 seasons.

Year	Treatment	Flowering Stage				Maturity Stage				
		Stem	Leaf	Glume	Total Biomass	Stem	Leaf	Glume	Grain	Total Biomass
2020–2021	CK	8352 ± 192 b	2349 ± 49 b	2572 ± 59 a	13,273 ± 105 b	6267 ± 70 b	1208 ± 14 c	3972 ± 45 a	9896 ± 111 cd	21,344 ± 240 a
	DI-H	8156 ± 303 bc	2406 ± 84 b	2623 ± 141 a	13,185 ± 187 b	6243 ± 481 b	1325 ± 102 bc	3073 ± 237 b	12,786 ± 985 a	23,426 ± 1805 a
	DI-M	7523 ± 726 cd	2678 ± 157 a	2573 ± 205 a	12,773 ± 508 b	5981 ± 173 bc	1522 ± 45 a	723 ± 21 e	12,901 ± 374 a	21,127 ± 613 a
	DI-L	6745 ± 65 e	2065 ± 212 cd	2219 ± 151 b	11,029 ± 212 c	4936 ± 255 d	1236 ± 64 bc	1279 ± 66 d	9400 ± 486 d	16,852 ± 871 b
	MS-H	10,456 ± 576 a	2356 ± 82 b	2495 ± 26 a	15,307 ± 479 a	8353 ± 751 a	941 ± 85 d	2518 ± 226 c	11,947 ± 1074 ab	23,759 ± 2135 a
	MS-M	8337 ± 283 b	2193 ± 93 bc	2547 ± 151 a	13,078 ± 251 b	6279 ± 183 b	1370 ± 40 b	2623 ± 76 c	11,008 ± 321 bc	21,280 ± 619 a
	MS-L	6855 ± 417 de	1885 ± 82 d	2128 ± 164 b	10,869 ± 555 c	5393 ± 666 cd	1006 ± 124 d	1271 ± 157 d	8975 ± 1109 d	16,645 ± 2058 b
2021–2022	CK	6102 ± 335 bc	1525 ± 85 c	2766 ± 384 bc	10,393 ± 785 bc	5693 ± 87 d	1026 ± 16 cd	1906 ± 29 b	9735 ± 148 d	18,360 ± 279 c
	DI-H	6981 ± 803 ab	1569 ± 161 bc	2811 ± 270 bc	11,361 ± 1198 ab	6456 ± 320 ab	1159 ± 57 b	1489 ± 74 c	12,140 ± 601 ab	21,243 ± 1052 a
	DI-M	7928 ± 1195 a	1609 ± 228 bc	3475 ± 541 a	13,012 ± 1962 a	6692 ± 170 a	1066 ± 27 c	569 ± 15 f	12,373 ± 315 a	20,700 ± 528 ab
	DI-L	5255 ± 521 c	1379 ± 79 c	2292 ± 391 c	8926 ± 948 c	4482 ± 97 f	894 ± 19 e	454 ± 10 g	8264 ± 179 e	14,094 ± 306 d
	MS-H	6439 ± 523 bc	1813 ± 144 ab	2927 ± 275 abc	11,179 ± 915 ab	6188 ± 258 bc	1287 ± 54 a	2651 ± 111 a	10,788 ± 451 c	20,915 ± 874 ab
	MS-M	7077 ± 201 ab	1913 ± 125 a	3031 ± 215 ab	12,021 ± 493 ab	6069 ± 263 c	1168 ± 51 b	819 ± 35 e	11,662 ± 506 b	19,718 ± 855 b
	MS-L	6253 ± 399 bc	1466 ± 79 c	2578 ± 230 bc	10,296 ± 705 bc	5084 ± 132 e	959 ± 25 de	1371 ± 36 d	9945 ± 258 d	17,360 ± 450 c

Note: different letters within the same column indicate significant differences at the 0.05 level among treatments within the same year.

3.4. The Response of Shoot Biomass Distribution and Harvest Index Distribution in Winter Wheat to Irrigation Methods and Regimes

During the flowering stage of winter wheat, the bulk of dry matter is primarily stored in the stems, while during maturity, it predominantly accumulates in the grains. Dry matter is primarily transferred from the stems to the grains during this stage (Table 6). With consistent irrigation methods, the harvest index (HI) of drip irrigation treatments displays an initial increase followed by a subsequent decrease as irrigation volume decreases, whereas the harvest index of micro-sprinkler irrigation rises with reduced irrigation volume. Comparatively, under the same irrigation regimen, the HI of drip irrigation treatments surpasses that of micro-sprinkler irrigation and significantly exceeds the control (CK), showing a remarkable 31.7% increase in the HI for the DI-M treatment in contrast to the CK.

Table 6. Stem (%), leaf (%), and glume (%) biomass distribution proportion and the harvest index (%) of winter wheat during the 2020–2022 seasons.

Year	Treatment	Flowering Stage			Maturity Stage			
		Stem	Leaf	Glume	Stem	Leaf	Glume	Harvest Index
2020–2021	CK	62.9 ± 1.0 b	17.7 ± 0.5 b	19.4 ± 0.6 a	29.4 ± 0.5 b	5.7 ± 0.2 b	18.6 ± 0.9 a	46.4 ± 0.7 f
	DI-H	61.8 ± 1.6 bc	18.2 ± 0.9 b	19.9 ± 1.1 a	28.0 ± 2.9 b	5.9 ± 0.3 b	13.8 ± 2.2 ab	57.3 ± 0.1 b
	DI-M	58.8 ± 3.8 c	21.0 ± 1.7 a	20.2 ± 2.2 a	28.3 ± 1.6 b	7.2 ± 0.6 a	3.4 ± 0.4 c	61.1 ± 3.4 a
	DI-L	61.2 ± 1.4 bc	18.7 ± 1.7 b	20.1 ± 1.2 a	29.3 ± 1.0 b	7.4 ± 0.4 a	7.6 ± 5.5 bc	55.8 ± 0.8 bc
	MS-H	68.3 ± 1.7 a	15.4 ± 1.0 c	16.3 ± 0.6 b	35.1 ± 2.1 a	3.9 ± 0.7 c	10.6 ± 6.4 abc	50.3 ± 2.8 e
	MS-M	63.8 ± 1.3 b	16.8 ± 0.4 bc	19.5 ± 1.4 a	29.5 ± 1.6 b	6.4 ± 1.0 ab	12.3 ± 3.1 ab	51.7 ± 0.4 de
	MS-L	63.1 ± 1.6 b	17.4 ± 0.8 bc	19.6 ± 1.0 a	32.4 a ± 4.9 b	6.0 ± 0.6 b	7.6 ± 7.8 bc	53.9 ± 0.7 cd
2021–2022	CK	58.8 ± 1.4 b	14.7 ± 0.4 bc	26.5 ± 1.7 a	31.8 ± 1.2 ab	5.6 ± 0.7 a	10.4 ± 0.4 b	53.0 ± 0.8 b
	DI-H	61.4 ± 0.9 a	13.8 ± 0.9 c	24.8 ± 0.3 a	32.6 ± 2.4 a	5.5 ± 0.7 a	7.0 ± 1.7 c	57.2 ± 2.9 a
	DI-M	60.9 ± 0.4 a	12.4 ± 0.2 d	26.7 ± 0.3 a	32.8 ± 0.0 a	5.2 ± 1.0 a	2.8 ± 0.9 d	59.8 ± 1.5 a
	DI-L	58.9 ± 1.5 b	15.5 ± 0.8 ab	25.6 ± 2.0 a	31.4 ± 1.6 ab	6.3 ± 0.6 a	3.2 ± 0.2 d	58.7 ± 1.3 a
	MS-H	57.6 ± 0.8 b	16.2 ± 0.1 a	26.2 ± 0.8 a	27.9 ± 3.0 b	6.1 ± 0.6 a	12.7 ± 0.7 a	51.6 ± 2.2 b
	MS-M	58.9 ± 0.8 b	15.9 ± 0.6 a	25.2 ± 0.9 a	29.2 ± 2.7 ab	5.9 ± 0.4 a	4.1 ± 1.3 d	59.2 ± 2.6 a
	MS-L	60.8 ± 0.5 a	14.3 ± 0.3 c	25.0 ± 0.5 a	30.2 ± 1.4 ab	5.5 ± 0.9 a	7.9 ± 1.6 c	57.3 ± 1.5 a

Note: different letters within the same column indicate significant differences at the 0.05 level among treatments within the same year.

3.5. The Response of Shoot Biomass Transfer and Its Contribution Rate to Grain of Winter Wheat to Irrigation Methods and Regimes

The patterns of biomass accumulation after flowering (BAF), biomass transfer amount (BTA), biomass transfer rate (BTR), and contribution rate of transferred biomass to grain (GCR) in winter wheat remain largely consistent across the two growing seasons, as depicted in Table 7. Within the same irrigation method, both drip irrigation and micro-sprinkler irrigation exhibit a decline in BAF with decreasing water application. In drip irrigation treatment, the BTA, BTR, and GCR initially rise before declining with increasing water deficit intensity, while in micro-sprinkler irrigation treatment, they demonstrate an increasing trend. When comparing irrigation regimes, there was no significant difference in BAF between drip irrigation and micro-sprinkler irrigation treatments. However, in mild and moderate water-deficient treatments, the BTA, BTR, and GCR were all higher than the CK ($p < 0.05$). Particularly, the DI-M treatment showed a significantly higher BTA, BTR, and GCR compared to the CK, with increases of 157.0%, 135.3%, and 114.9%, respectively ($p < 0.05$). In conclusion, under water deficit conditions, drip irrigation promotes the transfer of dry matter to grains, thereby enhancing its contribution to the grain formation process.

Table 7. Biomass translocation and its contribution rate of winter wheat during the 2020–2022 seasons.

Year	Treatment	BAF	BTA	BTR	GCR
		/kg·ha^{-1}	/kg·ha^{-1}	/%	/%
2020–2021	CK	8069 ± 149 a	1825 ± 90 d	13.8 ± 0.8 d	18.4 ± 1.1 e
	DI-H	9052 ± 1016 a	2538 ± 161 cd	19.3 ± 1.4 c	19.9 ± 1.5 de
	DI-M	8342 ± 370 a	4542 ± 441 a	35.6 ± 4.0 a	35.2 ± 3.9 ab
	DI-L	5793 ± 570 b	3571 ± 110 b	32.4 ± 1.9 ab	38.1 ± 2.3 a
	MS-H	8329 ± 1375 a	3512 ± 694 b	22.8 ± 3.1 c	29.3 ± 4.0 bc
	MS-M	8190 ± 381 a	2801 ± 167 bc	21.5 ± 1.9 c	25.5 ± 2.3 cd
	MS-L	6607 ± 1105 b	3241 ± 898 bc	29.4 ± 5.1 b	35.6 ± 6.2 a
2021–2022	CK	7964 ± 158 b	1771 ± 306 cd	17.0 ± 2.7 c	15.2 ± 2.4 d
	DI-H	9847 ± 563 a	2293 ± 1164 cd	19.9 ± 9.4 bc	16.7 ± 8.1 cd
	DI-M	7679 ± 332 bc	4694 ± 647 a	36.0 ± 4.0 a	36.2 ± 4.5 a
	DI-L	5164 ± 194 d	3101 ± 373 b	34.7 ± 3.4 a	35.5 ± 3.6 ab
	MS-H	9712 ± 467 a	1076 ± 918 d	9.4 ± 7.7 c	7.9 ± 6.5 d
	MS-M	7673 ± 521 bc	3989 ± 1027 ab	33.0 ± 7.0 a	31.9 ± 7.3 ab
	MS-L	7056 ± 267 c	2890 ± 525 b	28.0 ± 4.4 ab	25.5 ± 4.5 bc

Note: different letters within the same column indicate significant differences at the 0.05 level among treatments within the same year.

### 3.6. The Response of Nitrogen Uptake and Its Utilization of Winter Wheat to Irrigation Methods and Regimes

Drip irrigation shows a declining trend in plant nitrogen accumulation (NA) as irrigation volume decreases (Figure 4A), whereas nitrogen use efficiency (NUE) and nitrogen harvest index (NHI) initially rise and then fall with increasing water deficit intensity. Conversely, for micro-sprinkler irrigation, plant NA initially increases before decreasing with water deficit intensity, while NUE and NHI decrease initially and then increase with greater water deficit intensity (Figure 4B,C). Drip irrigation treatments generally exhibit higher NA compared to micro-sprinkler irrigation and the control group (CK). Furthermore, drip irrigation treatments with mild and moderate water deficit levels demonstrate higher NUE and NHI compared to micro-sprinkler irrigation treatments. Compared to the CK, NA increases by 32.9%, 15.6%, and 11.6% in the DI-H, DI-M, and MS-M treatments, respectively ($p < 0.05$). Similarly, NUE increases by 12.7%, 5.0%, 20.5%, and 8.0% in the DI-M, DI-L, MS-H, and MS-L treatments, respectively, compared to the CK ($p < 0.05$). Additionally, the NHI under different irrigation methods and strategies surpasses that of the CK treatment ($p < 0.05$; Figure 4C). It is evident that drip irrigation under well-watered conditions and mild water deficit situations demonstrates advantages in terms of nitrogen accumulation and utilization.
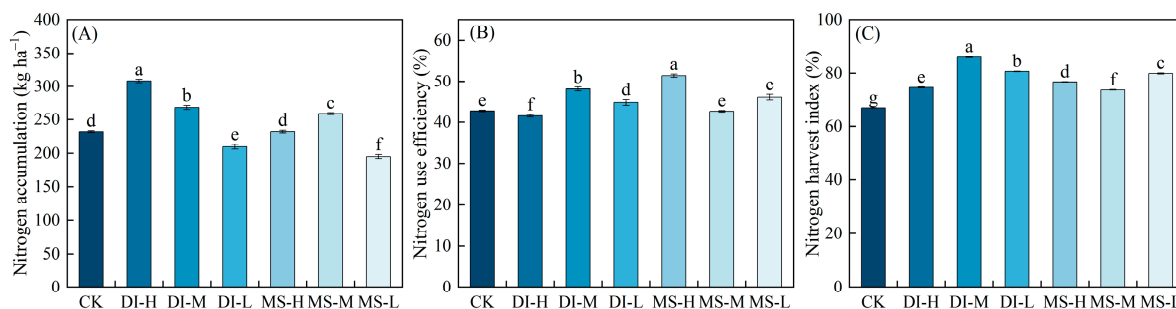
Figure 4. Nitrogen accumulation (NA, kg·ha^{-1}) (**A**), nitrogen use efficiency (NUE, %) (**B**), and nitrogen harvest index (NHI, %) (**C**) of winter wheat under different irrigation methods and regime treatments during the 2020–2021 seasons. (Note: different letters indicate significant differences at the 0.05 level. Error bars based on standard error (SE) were added to the data. Each data point was extended vertically by one standard error above and below the mean value).

3.7. Integrated Assessment of Irrigation Methods and Regime Strategies

Figure 5 presents the TOPSIS performance scores across different irrigation methods and regimes. In the 2020–2021 winter wheat season (Figure 5A), the TOPSIS score ranked as follows: DI-M > MS-H > DI-H > MS-M > DI-L > MS-L > CK, while in the 2021–2022 winter wheat season (Figure 5B), the order was DI-M > MS-M > DI-H > MS-L > DI-L > MS-H > CK. The normalized value radar chart further highlights that DI-M achieved the highest values for grain yield (GY), harvest index (HI), biomass transfer ability (BTA), biomass transfer rate (BTR), and grain-to-total biomass conversion rate (GCR) in both the 2020–2021 and 2021–2022 winter wheat seasons (Figure 5C,D). Overall, among all irrigation methods and regimes, DI-M emerges as the preferred choice for wheat under subsoiling fields due to its superior performance in grain yield, harvest index, and dry matter transfer rate.
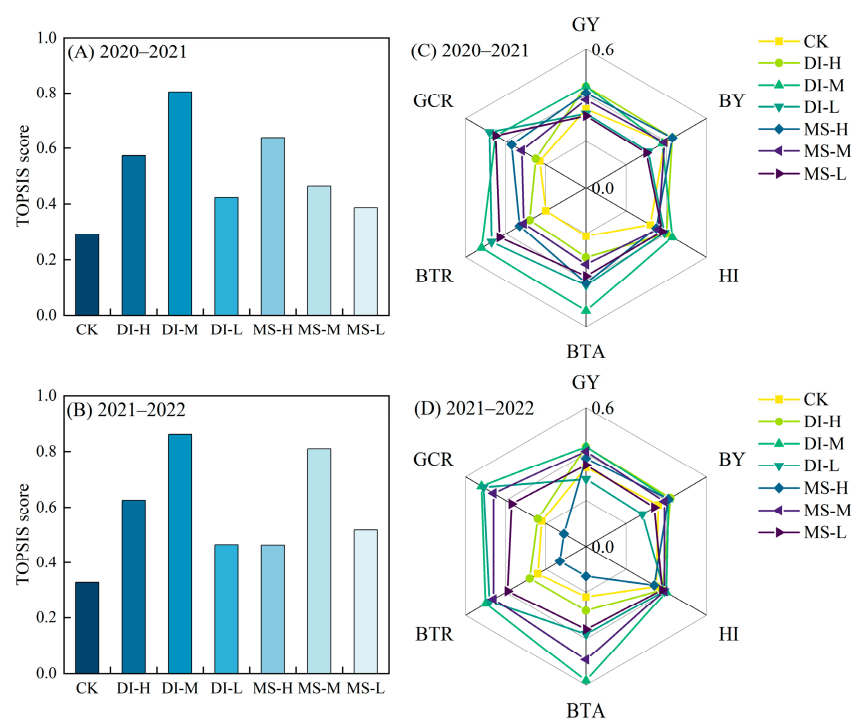
Figure 5. The TOPSIS scores for irrigation methods and regime treatments in the years 2020–2021 and 2021–2022 (**A**,**B**) along with the normalized values of all indicators for the same periods (**C**,**D**).

4. Discussion

4.1. Response of Plant Growth and Physiological Characteristics in Subsoiling Wheat Fields to Irrigation Methods and Regimes

Roots are pivotal organs for plants, providing essential anchorage in soil and enabling the absorption and transportation of water and nutrients crucial for growth and productivity. [30]. Research has consistently shown that as soil depth increases, the density of roots, particularly in terms of length, tends to decline [31,32]. In the context of this experiment, it was observed that roots predominantly occupied the upper 0–20 cm layer of soil, with root density gradually decreasing with greater soil depth (Figure 2). Notably, when comparing different irrigation methods, it was found that wheat roots exhibited a more robust response to drip irrigation in contrast to surface irrigation [33]. Across various soil layers, both drip and micro-sprinkler irrigation treatments demonstrated higher root dry weight density and bulk density within the 0–20 cm soil layer, particularly evident under conditions of water deficit in micro-sprinkler irrigation. Intriguingly, the application of water deficit treatment via micro-sprinkler irrigation appeared to stimulate deeper root growth in the 20–100 cm soil layer, indicating a positive effect on the deep root development of winter wheat [12]. The growth and development of roots have direct implications for the uptake of soil nutrients and water, thus exerting significant influence on aboveground plant growth [24]. Despite the promotion of root growth by water deficit, it was observed that such conditions tend to limit the growth of aboveground plant parts, leading to lower leaf area index (*LAI*) and *SPAD* values in winter wheat subjected to both drip and micro-sprinkler irrigation, consequently accelerating leaf senescence [34]. However, under conditions of adequate water supply in drip and micro-sprinkler irrigation systems, there was a reduction in root bulk density and dry weight density (Figure 2C,D), which, in turn, promoted aboveground plant growth. The *LAI* values recorded under both irrigation systems surpassed those of the control (CK) treatment (refer to Figure 1). Increasing the amount of irrigation to alleviate crop water deficit was found to significantly enhance the leaf area index of winter wheat, thereby preventing the decline in leaf photosynthetic rate associated with premature plant aging [35].

Photosynthesis, a fundamental physiological process for plants, is highly sensitive to water deficit, which can lead to constraints in leaf porosity, reduced gas exchange, and ultimately lower photosynthetic rates [36]. In line with the experiment's results, it was noted that leaf stomatal conductance, photosynthetic rate, and transpiration rate all declined as water deficit intensity increased. (Figure 3). The reduction in leaf water potential under conditions of water deficit prompted stomatal closure and decreased transpiration rates, consequently leading to diminished photosynthetic rates [35,37–39]. Furthermore, water deficit was found to suppress the downregulation of protein expression related to leaf photosynthesis and reduce leaf photosynthetic enzyme activity, thereby contributing to decreased photosynthetic rates due to non-stomatal leaf restrictions [40–43]. Consequently, there was an increasing trend in intercellular CO_2 concentration with rising water deficit intensity (refer to Figure 3B). Given the higher irrigation frequency and the suitability of soil water conditions associated with drip and micro-sprinkler irrigation in comparison to border irrigation [29,44], leaves under well-watered conditions in these systems exhibited significantly higher stomatal conductance, photosynthetic rates, and transpiration rates (see Figure 3).

4.2. Response of Dry Matter Transfer and Nitrogen Allocation to Irrigation Methods and Regimes in Subsoiling Wheat Fields

Plant leaves represent the organs with the highest efficiency in photosynthesis, serving as a crucial source of carbohydrates essential for grain development [45]. However, water deficit conditions impose constraints on photosynthesis, resulting in a significant reduction in carbon absorption and utilization capacity, ultimately impacting crop dry matter accumulation and leading to decreased grain yield [45,46]. The distribution and transport of dry matter are pivotal for achieving high and stable wheat yields [47]. Particularly, post-anthesis dry matter accumulation plays a critical role in grain yield, accounting for 60–90% of the final grain yield. However, when water deficit conditions occur, post-anthesis dry matter accumulation typically diminishes, resulting in considerable yield losses [48–51]. In the context of this experiment, moderate water scarcity led to decreased dry matter mass and grain yield during both flowering and maturation stages, along with a notable reduction in grain dry matter distribution and post-flowering dry matter transfer. Consequently, there was a significant increase in the contribution rate of pre-flowering dry matter transfer to grains. In comparison with adequately irrigated (H) treatment, moderate water scarcity (L) irrigation led to a decrease in grain yield by 29.2% and 16.3% ($p < 0.05$). Hence, maintaining appropriate soil moisture levels is beneficial for enhancing post-flowering dry matter accumulation and, subsequently, increasing yield [52]. Different rates of soil evapotranspiration under various irrigation methods result in discrepancies in soil water distribution, further influencing the process of dry matter accumulation and transfer [47,53]. Research has indicated that drip irrigation can enhance post-flowering dry matter accumulation in wheat, significantly improving grain yield and water use efficiency [54]. Consistently, the experiment revealed that the amount of dry matter transfer, grain yield, and harvest index under drip and micro-sprinkler irrigation treatments were significantly higher compared to border irrigation treatment, with particularly notable outcomes under slight deficit (M) conditions (refer to Tables 6 and 7). The utilization efficiency of slight water deficit and water scarcity in drip irrigation was notably superior to that of micro-sprinkler irrigation [29], suggesting that drip irrigation is more conducive to enhancing crop grain yield and water productivity [55]. Given the frequent irrigation associated with drip systems, surface soil moisture tends to be more conducive, promoting nitrogen uptake by plants and subsequently increasing crop yield [55–57]. Nitrogen accumulation in the DI-H treatment increased by 32.9% and 32.7% compared with CK and MS-H ($p < 0.05$), while the nitrogen use efficiency and nitrogen harvest index of the DI-M treatment were notably higher than the CK treatment, increasing by 12.7% and 28.7%, respectively ($p < 0.05$). This indicates that drip irrigation enhances total nitrogen accumulation in plants, thereby improving crop nitrogen use efficiency and overall nitrogen utilization [12,58]. A comprehensive evaluation

using TOPSIS methodology concluded that the overall scores of drip and micro-sprinkler irrigation under mild water deficit (60%FC) were higher, which was consistent with the findings of Mehmood et al. [59]. Drip irrigation under a 60%FC irrigation plan exhibited the most significant impact on yield improvement and nitrogen utilization. Considering various factors, such as grain yield, dry matter transfer, water and nitrogen utilization, and economic benefits, the 60%FC drip irrigation method is deemed the optimal choice for winter wheat in the Huang–Huai–Hai Plain [29].

5. Conclusions

This study highlights the importance of winter wheat cultivation in subsoiled fields, particularly emphasizing the role of irrigation methods and regimes. Drip irrigation, especially with mild water deficit (60%FC), enhances root growth, nutrient uptake, and post-flowering dry matter accumulation, resulting in higher grain yield and water productivity compared to surface irrigation and micro-sprinkler irrigation. Efficient nitrogen management alongside drip irrigation further boosts nitrogen utilization efficiency and crop yields. Considering economic factors, adopting drip irrigation with mild water deficit emerges as the optimal approach for maximizing winter wheat production in the North China Plain, offering improved resource utilization and economic returns.

Abbreviations

DI, drip irrigation; MS, micro-sprinkler irrigation; *LAI*, leaf area index; C_i, intercellular CO_2 concentration ($\mu mol \cdot s^{-1}$); G_s, stomatal conductance ($mol \cdot m^{-2} \cdot s^{-1}$); P_n, net photosynthetic rate ($\mu mol \cdot m^{-2} \cdot s^{-1}$); T_r, transpiration rate ($mmol \cdot m^{-2} \cdot s^{-1}$); BAF, biomass accumulation after flowering ($kg \cdot ha^{-1}$); BTA, biomass transfer amount ($kg \cdot ha^{-1}$); BTR, biomass transfer rate (%); GCR, contribution rate of transferred biomass to grain (%); NA, nitrogen accumulation ($kg \cdot ha^{-1}$); NUE, nitrogen use efficiency (%); NHI, nitrogen harvest index (%).

References

1. Keller, T.; Sandin, M.; Colombi, T.; Horn, R.; Or, D. Historical increase in agricultural machinery weights enhanced soil stress levels and adversely affected soil functioning. *Soil. Tillage Res.* **2019**, *194*, 104293. [CrossRef]

2. Sun, Q.; Sun, W.; Zhao, Z.X.; Jiang, W.; Zhang, P.Y.; Sun, X.F.; Xue, Q.W. Soil Compaction and Maize Root Distribution under Subsoiling Tillage in a Wheat–Maize Double Cropping System. *Agronomy* **2023**, *13*, 394. [CrossRef]

3. Liu, X.W.; Zhang, X.Y.; Chen, S.Y.; Sun, H.Y.; Shao, L.W. Subsoil compaction and irrigation regimes affect the root-shoot relationship and grain yield of winter wheat. *Agric. Water Manag.* **2015**, *154*, 59–67. [CrossRef]

4. Zhang, X.Y.; Shao, L.W.; Sun, H.Y.; Chen, S.Y.; Wang, Y.Z. Incorporation of Soil Bulk Density in Simulating Root Distribution of Winter Wheat and Maize in Two Contrasting Soils. *Soil. Sci. Soc. Am. J.* **2012**, *76*, 638–647. [CrossRef]

5. Boomsma, C.R.; Santini, J.B.; West, T.D.; Brewer, J.C.; McIntyre, L.M.; Vyn, T.J. Maize grain yield responses to plant height variability resulting from crop rotation and tillage system in a long-term experiment. *Soil. Tillage Res.* **2010**, *106*, 227–240. [CrossRef]

6. Tolon-Becerra, A.; Tourn, M.; Botta, G.F.; Lastra-Bravo, X. Effects of different tillage regimes on soil compaction, maize (L.) seedling emergence and yields in the eastern Argentinean Pampas region. *Soil. Tillage Res.* **2011**, *117*, 184–190. [CrossRef]

7. Nele, V.; Victoria, N.; Niels, J.; Heleen, H.; Ken, D.S.; Dirk, R.; Seppe, D.; Bram, G. Soil water content, maize yield and its stability as affected by tillage and crop residue management in rainfed semi-aridhighlands. *Plant Soil.* **2011**, *344*, 73–85. [CrossRef]

8. Jennings, T.N.; Smith, J.E.; Cromack, K.; Sulzman, E.W.; McKay, D.; Caldwell, B.A.; Beldin, S.I. Impact of postfire logging on soil bacterial and fungal communities and soil biogeochemistry in a mixed-conifer forest in central Oregon. *Plant Soil.* **2012**, *350*, 393–411. [CrossRef]

9. Massa, D.; Magán, J.J.; Montesano, F.F.; Tzortzakis, N. Review Minimizing water and nutrient losses from soilless cropping in southern Europe. *Agric. Water Manag.* **2020**, *241*, 106395. [CrossRef]

10. Tian, X.M.; Fan, H.; Wang, J.Q.; Ippolito, J.; Li, Y.B.; Feng, S.S.; An, M.J.; Zhang, F.H.; Wang, K.Y. Effect of polymer materials on soil structure and organic carbon under drip irrigation. *Geoderma* **2019**, *340*, 94–103. [CrossRef]

11. Jha, S.K.; Ramatshaba, T.S.; Wang, G.S.; Liang, Y.P.; Liu, H.; Gao, Y.; Duan, A. Response of growth, yield and water use efficiency of winter wheat to different irrigation methods and scheduling in North China Plain. *Agric. Water Manag.* **2019**, *217*, 292–302. [CrossRef]

12. Li, J.P.; Xu, X.X.; Lin, G.; Wang, Y.Q.; Liu, Y.; Zhang, M.; Zhou, J.Y.; Wang, Z.M.; Zhang, Y.H. Micro-irrigation improves grain yield and resource use efficiency by co-locating the roots and N-fertilizer distribution of winter wheat in the North China Plain. *Sci. Total Environ.* **2018**, *643*, 367–377. [CrossRef]

13. Fang, Q.; Zhang, X.Y.; Shao, L.W.; Chen, S.Y.; Sun, H.Y. Assessing the performance of different irrigation systems on winter wheat under limited water supply. *Agric. Water Manag.* **2018**, *196*, 133–143. [CrossRef]

14. Cao, Y.X.; Cai, H.J.; Sun, S.K. Effects of growth-stage-based limited irrigation management on the growth, yields, and radiation utilization efficiency of winter wheat in northwest China. *J. Sci. Food Agric.* **2021**, *101*, 5819–5826. [CrossRef]

15. Li, J.P.; Wang, Z.M.; Yao, C.S.; Zhang, Z.; Liu, Y.; Zhang, Y.H. Micro-sprinkling irrigation simultaneously improves grain yield and protein concentration of winter wheat in the North China Plain. *Crop J.* **2021**, *9*, 1397–1407. [CrossRef]

16. Yan, S.C.; Wu, Y.; Fan, J.L.; Zhang, F.C.; Guo, J.J.; Zheng, J.; Wu, L.F. Quantifying grain yield, protein, nutrient uptake and utilization of winter wheat under various drip fertigation regimes. *Agric. Water Manag.* **2022**, *261*, 107380. [CrossRef]

17. Hao, T.J.; Zhu, Z.X.; Zhang, Y.L.; Liu, S.; Xu, Y.F.; Xu, X.X.; Zhao, C.X. Effects of Drip Irrigation and Fertilization Frequency on Yield, Water and Nitrogen Use Efficiency of Medium and Strong Gluten Wheat in the Huang-Huai-Hai Plain of China. *Agronomy* **2023**, *13*, 1564. [CrossRef]

18. Bai, S.S.; Wan, S.Q.; Kang, Y.H. Winter wheat growth and water use under different micro-sprinkling irrigation regimes in the North China Plain. *Paddy Water Environ.* **2020**, *18*, 561–571. [CrossRef]

19. Zhang, J.M.; Wu, J.C.; Yang, Y.H.; Pan, X.Y.; Wang, Y.; He, F. Effect of different irrigation technology on yield and water use efficiency of wheat. *Water Sav. Irrig.* **2016**, *30*–*32*, 37.

20. Lv, H.F.; Lin, S.; Wang, Y.F.; Lian, X.J.; Zhao, Y.M.; Li, Y.J.; Du, J.Y.; Wang, Z.X.; Wang, J.G.; Butterbach-Bahl, K. Drip fertigation significantly reduces nitrogen leaching in solar green house vegetable production system. *Environ. Pollut.* **2019**, *245*, 694–701. [CrossRef]

21. Amirahmadi, E.; Ghorbani, M.; Moudrý, J.; Bernas, J.; Mukosha, C.E.; Hoang, T.N. Environmental Assessment of Dryland and Irrigated Winter Wheat Cultivation under Compost Fertilization Strategies. *Plants* **2024**, *13*, 509. [CrossRef]

22. Li, H.R.; Mei, X.R.; Wang, J.D.; Huang, F.; Hao, W.P.; Li, B.G. Drip fertigation significantly increased crop yield, water productivity and nitrogen use efficiency with respect to traditional irrigation and fertilization practices: A meta-analysis in China. *Agric. Water Manag.* **2021**, *244*, 106534. [CrossRef]

23. Sharmasarkar, C.F.; Sharmasarkar, S.; Miller, S.D.; Vance, G.F.; Zhang, R. Assessment of drip and flood irrigation on water and fertilizer use efficiencies for sugarbeets. *Agric. Water Manag.* **2001**, *46*, 241–251. [CrossRef]

24. Dehghanisanij, H.; Kouhi, N. Effects of Nitrogen and Drip Irrigation Rates on Root Development of Corn (*Zea mays* L.) and Residual Soil Moisture. *Gesunde Pflanz.* **2020**, *72*, 335–349. [CrossRef]

25. *GB/T17296-2009*; China Soil Classification and Code. National Standards of China (NSC): Beijing, China, 2009.

26. Fan, Y.L.; Ma, Y.Z.; Zaman, A.M.; Zhang, M.M.; Li, Q. Delayed irrigation at the jointing stage increased the post-flowering dry matter accumulation and water productivity of winter wheat under wide-precision planting pattern. *J. Sci. Food Agric.* **2023**, *103*, 1925–1934. [CrossRef]

27. Garcia-Servin, M.; Contreras-Medina, L.M.; Torres-Pacheco, I.; Guevara-González, R.G. Estimation of Nitrogen Status in Plants. *Nitrate Handb.* **2022**, *1*, 163–181. [CrossRef]

28. Qi, D.; Pan, C. Responses of shoot biomass accumulation, distribution, and nitrogen use efficiency of maize to nitrogen application rates under waterlogging. *Agric. Water Manag.* **2022**, *261*, 107352. [CrossRef]

29. Liu, X.; Liu, J.; Huang, C.; Liu, H.; Meng, Y.; Chen, H.; Ma, S.; Liu, Z. The impacts of irrigation methods and regimes on the water and nitrogen utilization efficiency in subsoiling wheat fields. *Agric. Water Manag.* **2024**, *295*, 108765. [CrossRef]

30. Chilundo, M.; Joel, A.; Wesstrom, I.; Brito, R.; Messing, I. Response of maize root growth to irrigation and nitrogen management strategies in semi-arid loamy sandy soil. *Field Crop Res.* **2017**, *200*, 143–162. [CrossRef]

31. Mahgoub, N.A.; Ibrahim, A.M.; Ali, O.M. Effect of different irrigation systems on root growth of maize and cowpea plants in sandy soil. *Eurasian Soil. Sci.* **2017**, *6*, 374–379. [CrossRef]

32. Firouzabadi, A.G.; Baghani, J.; Jovzi, M.; Albaji, M. Effects of wheat row spacing layout and drip tape spacing on yield and water productivity in sandy clay loam soil in a semi-arid region. *Agric. Water Manag.* **2021**, *251*, 106868. [CrossRef]

33. Kaur, T.; Sharma, P.K.; Brar, A.S.; Vashisht, B.B.; Choudhary, A.K. Optimizing crop water productivity and delineating root architecture and water balance in cotton–wheat cropping system through sub-surface drip irrigation and foliar fertilization strategy in an alluvial soil. *Field Crop Res.* **2024**, *309*, 109337. [CrossRef]

34. Stone, P.J.; Wilson, D.R.; Jamieson, P.D.; Gillespie, R.N. Water deficit effects on sweet corn. II. Canopy development. *Aust. J. Agric. Res.* **2001**, *52*, 115–126. [CrossRef]

35. Li, H.Q.; Zhang, M.Z.; Xiao, N.; Yang, H.J. Different Deficit Irrigation Lower Limits and Irrigation Quotas Affect the Yield and Water Use Efficiency of Winter Wheat by Regulating Photosynthetic Characteristics. *Phyton Int. J. Exp. Bot.* **2023**, *92*, 3211–3236. [CrossRef]

36. Lawlor, D.W.; Cornic, G. Photosynthetic carbon assimilation and associated metabolism in relation to water deficits in higher plants. *Plant Cell Environ.* **2002**, *25*, 275–294. [CrossRef] [PubMed]

37. Lang, Y.; Wang, M.; Zhang, G.C.; Zhao, Q.K. Experimental and simulated light responses of photosynthesis in leaves of three tree species under different soil water conditions. *Photosynthetica* **2013**, *51*, 370–378. [CrossRef]

38. Yang, J.C.; Zhang, J.H.; Huang, Z.L.; Zhu, Q.S.; Wang, L. Remobilization of carbon reserves is improved by controlled soil-drying during grain filling of wheat. *Crop Sci.* **2000**, *40*, 1645–1655. [CrossRef]

39. Wu, Y.L.; Guo, Q.F.; Luo, Y.; Tian, F.X.; Wang, W. Differences in physiological characteristics between two wheat cultivars exposed to field water deficit conditions. *Russ. J. Plant Physl.* **2014**, *61*, 451–459. [CrossRef]

40. Zong, Y.Z.; Shangguan, Z.P. Nitrogen Deficiency Limited the Improvement of Photosynthesis in Maize by Elevated CO_2 under Drought. *J. Integr. Agric.* **2014**, *13*, 73–81. [CrossRef]

41. Perdomo, J.A.; Capó-Bauçà, S.; Carmo-Silva, E.; Galmés, J. Rubisco and Rubisco Activase Play an Important Role in the Biochemical Limitations of Photosynthesis in Rice, Wheat, and Maize under High Temperature and Water Deficit. *Front. Plant Sci.* **2017**, *8*, 490. [CrossRef]

42. Zhang, X.; Pu, P.; Tang, Y.; Zhang, L.X.; Lv, J.Y. C4 photosynthetic enzymes play a key role in wheat spike bracts primary carbon metabolism response under water deficit. *Plant Physiol. Bioch.* **2019**, *142*, 163–172. [CrossRef] [PubMed]

43. Zhu, D.; Zhu, G.R.; Zhang, Z.; Wang, Z.M.; Yan, X.; Yan, Y.M. Effects of Independent and Combined Water-Deficit and High-Nitrogen Treatments on Flag Leaf Proteomes during Wheat Grain Development. *Int. J. Mol. Sci.* **2020**, *21*, 2098. [CrossRef] [PubMed]

44. Guo, X.L.; Zhao, Q.; Li, J.Y.; Wang, Z.M.; Zhang, Y.H.; Xue, X.Z. Daily drip irrigation based on real-time weather improves winter wheat grain yield and water use efficiency. *Irrig. Drain.* **2022**, *71*, 589–603. [CrossRef]

45. Luo, F.; Deng, X.; Liu, Y.; Yan, Y.M. Identification of phosphorylation proteins in response to water deficit during wheat flag leaf and grain development. *Bot. Stud.* **2018**, *59*, 28. [CrossRef] [PubMed]

46. Reddy, A.R.; Chaitanya, K.V.; Vivekanandan, M. Drought-induced responses of photosynthesis and antioxidant metabolism in higher plants. *J. Plant Physiol.* **2004**, *161*, 1189–1202. [CrossRef] [PubMed]

47. Ding, J.F.; Zi, Y.; Li, C.Y.; Peng, Y.X.; Zhu, X.K.; Guo, W.S. Dry Matter Accumulation, Partitioning, and Remobilization in High-Yielding Wheat under Rice-Wheat Rotation in China. *Agron. J.* **2016**, *108*, 604–614. [CrossRef]

48. Masoni, A.; Ercoli, L.; Mariotti, M.; Arduini, I. Post-anthesis accumulation and remobilization of dry matter, nitrogen and phosphorus in durum wheat as affected by soil type. *Eur. J. Agron.* **2007**, *26*, 179–186. [CrossRef]

49. Yang, J.C.; Zhang, J.H. Grain filling of cereals under soil drying. *New Phytol.* **2006**, *169*, 223–236. [CrossRef]

50. Koutroubas, S.D.; Fotiadis, S.; Damalas, C.A. Biomass and nitrogen accumulation and translocation in spelt (*Triticum spelta*) grown in a Mediterranean area. *Field Crop Res.* **2012**, *127*, 1–8. [CrossRef]

51. Yan, S.C.; Wu, Y.; Fan, J.L.; Zhang, F.C.; Guo, J.J.; Zheng, J.; Wu, L.F. Optimization of drip irrigation and fertilization regimes to enhance winter wheat grain yield by improving post-anthesis dry matter accumulation and translocation in northwest China. *Agric. Water Manag.* **2022**, *271*, 107782. [CrossRef]

52. Fang, Y.; Liang, L.Y.; Liu, S.; Xu, B.C.; Siddique, K.H.; Palta, J.A.; Chen, Y.L. Wheat cultivars with small root length density in the topsoil increased post-anthesis water use and grain yield in the semi-arid region on the Loess Plateau. *Eur. J. Agron.* **2021**, *124*, 126243. [CrossRef]

53. Wu, X.; Zhang, W.J.; Liu, W.; Zuo, Q.; Shi, J.C.; Yan, X.D.; Zhang, H.F.; Xue, X.Z.; Wang, L.C.; Zhang, M.; et al. Root-weighted soil water status for plant water deficit index based irrigation scheduling. *Agric. Water Manag.* **2017**, *189*, 137–147. [CrossRef]

54. Ma, S.T.; Meng, Y.; Han, Q.S.; Ma, S.C. Drip fertilization improve water and nitrogen use efficiency by optimizing root and shoot traits of winter wheat. *Front. Plant Sci.* **2023**, *14*, 1201966. [CrossRef] [PubMed]

55. Lu, J.S.; Geng, C.M.; Cui, X.L.; Li, M.Y.; Chen, S.H.; Hu, T.T. Response of drip fertigated wheat-maize rotation system on grain yield, water productivity and economic benefits using different water and nitrogen amounts. *Agric. Water Manag.* **2021**, *258*, 107220. [CrossRef]

56. Lv, G.H.; Kang, Y.H.; Li, L.; Wan, S.Q. Effect of irrigation methods on root development and profile soil water uptake in winter wheat. *Irr. Sci.* **2010**, *28*, 387–398. [CrossRef]

57. Ehdaie, B.; Merhaunt, D.J.; Ahmadian, S. Root system size influences water-nutrient uptake and nitrate leaching potential in wheat. *J. Agron. Crop Sci.* **2010**, *196*, 455–466. [CrossRef]

58. Surendran, U.; Madhava, C.K. Development and evaluation of drip irrigation and fertigation scheduling to improve water productivity and sustainable crop production using HYDRUS. *Agric. Water Manag.* **2022**, *269*, 107668. [CrossRef]

59. Mehmood, F.; Wang, G.S.; Abubakar, S.A.; Zain, M.; Rahman, S.U.; Gao, Y.; Duan, A.W. Optimizing irrigation management sustained grain yield, crop water productivity, and mitigated greenhouse gas emissions from the winter wheat field in North China Plain. *Agric. Water Manag.* **2023**, *290*, 108599. [CrossRef]